Phases of QCD: lattice thermodynamics and a field theoretical model[*]

Claudia Ratti[a,b], Michael A. Thaler[a] and Wolfram Weise[a]

[a]Physik-Department, Technische Universität München, D-85747 Garching, Germany

[b]ECT*, I-38050 Villazzano (Trento), Italy

(Email: Claudia_Ratti@ph.tum.de, Michael_Thaler@ph.tum.de, Wolfram_Weise@ph.tum.de)

November 26, 2024

Abstract

We investigate three-colour QCD thermodynamics at finite quark chemical potential. Lattice QCD results are compared with a generalized Nambu Jona-Lasinio model in which quarks couple simultaneously to the chiral condensate and to a background temporal gauge field representing Polyakov loop dynamics. This so-called PNJL model thus includes features of both deconfinement and chiral symmetry restoration. The parameters of the Polyakov loop effective potential are fixed in the pure gauge sector. The chiral condensate and the Polyakov loop as functions of temperature and quark chemical potential are calculated by minimizing the thermodynamic potential of the system. The resulting equation of state, (scaled) pressure difference and quark number density at finite quark chemical potential are then confronted with corresponding Lattice QCD data.

PACS: 12.38.Aw, 12.38.Mh

---

1 Introduction

Recent years have seen an expansion of activities devoted to the study of the QCD phase diagram. Heavy-ion experiments are looking for signals of the Quark-Gluon Plasma. Large-scale lattice simulations at finite temperature have become a principal tool for investigating the pattern of phases in QCD. Accurate computations of lattice QCD thermodynamics in the pure gauge sector have been performed. First results at finite quark chemical potential are available. The equation of state of strongly interacting matter is now at hand as a function of temperature T and in a limited range of quark chemical potential μ. Improved multi-parameter re-weighting techniques [1, 2], Taylor series expansion methods [3–5] and analytic continuation from imaginary chemical potential [6–9] provide lattice data for the pressure, entropy density, quark density and selected susceptibilities.

A straightforward interpretation of these data in terms of QCD perturbation theory does not work because of poor convergence at any temperature of practical interest [10, 11]. In order to overcome this problem, resummation schemes have been proposed, based for example on the Hard Thermal Loop (HTL) approach [12–20] or on dimensionally reduced screened perturbation theory (DRSPT) [21–23]. However, these approaches still give reliable results only for temperatures $T \gtrsim 2.5\,T_c$, far above the critical temperature $T_c \sim 0.2$ GeV. At these high temperatures, the HTL approach motivates and justifies a picture of weakly interacting quasiparticles, as determined by the HTL propagators.

In order to extend such descriptions to lower temperatures closer to T_c, various models have been proposed. Early attempts were based on the MIT bag model [24]. More sophisticated approaches became necessary when more precise lattice data appeared. Various aspects of QCD thermodynamics have been investigated in terms of quasiparticle models based on perturbative calculations carried out in the HTL scheme [25–30], in terms of a condensate of Z_3 Wilson lines [31], by refined quasiparticle models based on the HTL-resummed entropy and extensions thereof [32], by an improved version with a temperature-dependent number of active degrees of freedom [33, 34], by an evaporation model of the gluon condensate [35], by quasiparticle models formulated in dynamical terms [36], and by hadron resonance gas models below the critical temperature [37] (for a recent review see [38]).

In this paper, we study the thermodynamics of two-flavour QCD at finite quark chemical potential. Our investigation is based on a synthesis of a Nambu Jona-Lasinio (NJL) model [39–44] and the non-linear dynamics involving the Polyakov loop [45–49]. In this Polyakov-loop-extended (PNJL) model, quarks develop quasiparticle masses by propagating in the chiral condensate, while they couple at the same time to a homogeneous background (temporal) gauge field representing Polyakov loop dynamics.

The "classic" NJL model incorporates the chiral symmetry of two-flavour QCD

and its spontaneous breakdown at $T < T_c$. Gluonic degrees of freedom are "integrated out" and replaced by a local four-point interaction of quark colour currents. Subsequent Fierz transformations project this interaction into various quark-antiquark and diquark channels. The colour singlet $q\bar{q}$ modes of lowest mass are identified with the lightest mesons. Pions properly emerge as Goldstone bosons at $T < T_c$. However, the local $SU(N_c)$ gauge invariance of QCD is now replaced by a global $SU(N_c)$ symmetry in the NJL model, so that the confinement property is lost. Consequently, standard NJL-type models are bound to fail in attempts to describe $N_c = 3$ thermodynamics around T_c (and beyond) for non-zero quark chemical potential μ.

On the other hand the NJL model, with just the simplest possible one-parameter colour current-current interaction between quarks, is remarkably successful in reproducing the thermodynamics of $N_c = 2$ Lattice QCD at finite μ [50]. Encouraged by this result, the NJL quasiparticle concept does suggest itself as a useful starting point. However, whereas aspects of deconfinement are less significant in the $N_c = 2$ case, they figure prominently for $N_c = 3$. This motivates our extension towards the PNJL Lagrangian as a minimal approach incorporating both chiral symmetry restoration and deconfinement.

The deconfinement phase transition is well defined in the heavy-quark limit, where the Polyakov loop serves as an order parameter. This phase transition is characterized by the spontaneous breaking of the $Z(3)$ center symmetry of QCD [51–54]. In the presence of dynamical quarks the center symmetry is explicitly broken. No order parameter is established for the deconfinement transition in this case [55], but the Polyakov loop still serves as an indicator of a rapid crossover towards deconfinement. The chiral phase transition, on the other hand, has a well-defined order parameter in the chiral limit of massless quarks: the chiral (or quark) condensate $\langle \bar{q}q \rangle$. This condensate, and its dynamical generation, is the basic element of the original NJL model.

The primary aim of this paper is to test the effectiveness of the PNJL approach when confronted with Lattice QCD thermodynamics. The PNJL Lagrangian is derived in Section 2. Parameters are fixed in Section 3 by reproducing known properties of the pion and of the QCD vacuum in the hadronic phase, while the Polyakov loop effective potential is adjusted to pure gauge lattice results. Sections 4 and 5 deal with the thermodynamics derived from the PNJL Lagrangian in the mean-field approximation. This discussion includes a detailed comparison with Lattice QCD results at zero and at finite chemical potential.

2 The PNJL model

Following [47] we introduce a generalized $N_f = 2$ Nambu Jona-Lasinio Lagrangian with quarks coupled to a (spatially constant) temporal background gauge field representing Polyakov loop dynamics (the PNJL model):

$$\mathcal{L}_{PNJL} = \bar{\psi} \left(i\gamma_\mu D^\mu - \hat{m}_0 \right) \psi + \frac{G}{2} \left[\left(\bar{\psi}\psi \right)^2 + \left(\bar{\psi} i\gamma_5 \vec{\tau}\psi \right)^2 \right] - \mathcal{U} \left(\Phi[A], \bar{\Phi}[A], T \right), \quad (1)$$

where $\psi = (\psi_u, \psi_d)^T$ is the quark field,

$$D^\mu = \partial^\mu - iA^\mu \qquad \text{and} \qquad A^\mu = \delta_{\mu 0} A^0 \quad . \qquad (2)$$

The gauge coupling g is conveniently absorbed in the definition of $A^\mu(x) = g\mathcal{A}_a^\mu(x)\frac{\lambda_a}{2}$ where $\mathcal{A}_a^\mu$ is the SU(3) gauge field and λ_a are the Gell-Mann matrices. The two-flavour current quark mass matrix is $\hat{m}_0 = diag(m_u, m_d)$ and we shall work in the isospin symmetric limit with $m_u = m_d \equiv m_0$. A local, chirally symmetric scalar-pseudoscalar four-point interaction of the quark fields is introduced with an effective coupling strength G.

The quantity $\mathcal{U}(\Phi, \bar{\Phi}, T)$ is the effective potential expressed in terms of the traced Polyakov loop[1] and its (charge) conjugate,

$$\Phi = (\text{Tr}_c L)/N_c, \qquad\qquad \bar{\Phi} = (\text{Tr}_c L^\dagger)/N_c. \qquad (3)$$

The Polyakov loop L is a matrix in colour space explicitly given by

$$L(\vec{x}) = \mathcal{P} \exp \left[i \int_0^\beta d\tau \, A_4 (\vec{x}, \tau) \right], \qquad (4)$$

with $\beta = 1/T$ the inverse temperature and $A_4 = iA^0$. In a convenient gauge (the so-called Polyakov gauge), the Polyakov loop matrix can be given a diagonal representation [47].

The coupling between Polyakov loop and quarks is uniquely determined by the covariant derivative D_μ in the PNJL Lagrangian (1). Note that in the chiral limit ($\hat{m}_0 \to 0$), this Lagrangian is invariant under the chiral flavour group, $SU(2)_L \times SU(2)_R$, just like the original QCD Lagrangian.

The trace of the Polyakov loop, Φ, and its conjugate, $\bar{\Phi}$, will be treated as classical field variables throughout this work. In the absence of quarks, we have $\Phi = \bar{\Phi}$ and the Polyakov loop serves as an order parameter for deconfinement. The phase transition is characterized by the spontaneous breaking of the $Z(3)$ center symmetry of QCD. The temperature dependent effective potential $\mathcal{U}$ has the following general features. At low temperatures, $\mathcal{U}$ has a single minimum at Φ=0, while at high

---

[1]more precisely: the Polyakov line with periodic boundary conditions

temperatures it develops a second one which turns into the absolute minimum above a critical temperature T_0. In the limit $T \to \infty$ we have $\Phi \to 1$. The function $\mathcal{U}(\Phi, \bar{\Phi}, T)$ will be fixed by comparison with pure-gauge Lattice QCD. We choose the following general form in accordance with the underlying $Z(3)$ symmetry:

$$\frac{\mathcal{U}\left(\Phi, \bar{\Phi}, T\right)}{T^4} = -\frac{b_2\left(T\right)}{2}\bar{\Phi}\Phi - \frac{b_3}{6}\left(\Phi^3 + \bar{\Phi}^3\right) + \frac{b_4}{4}\left(\bar{\Phi}\Phi\right)^2 \qquad (5)$$

with

$$b_2\left(T\right) = a_0 + a_1\left(\frac{T_0}{T}\right) + a_2\left(\frac{T_0}{T}\right)^2 + a_3\left(\frac{T_0}{T}\right)^3 . \qquad (6)$$

A precision fit of the coefficients a_i, b_i is performed to reproduce the lattice data (see section 3).

Using standard bosonization techniques the Lagrangian (1) can be rewritten in terms of the auxiliary field variables σ and $\vec{\pi}$:

$$\mathcal{L}_{eff} = -\frac{\sigma^2 + \vec{\pi}^2}{2G} - \mathcal{U}\left(\Phi, \bar{\Phi}, T\right) - i\mathrm{Tr}\ln S^{-1}, \qquad (7)$$

where an irrelevant constant has been dropped and

$$S^{-1} = i\gamma_\mu\partial^\mu - \gamma_0 A^0 - \hat{M} \qquad (8)$$

is the inverse quark propagator with

$$\hat{M} = \hat{m}_0 - \sigma - i\gamma_5\vec{\tau}\cdot\vec{\pi}. \qquad (9)$$

The trace in (7) is taken over colour, flavour and Dirac indices. The field equations for σ, $\vec{\pi}$, Φ and $\bar{\Phi}$ are then solved in the mean field approximation[2]. The expectation value $\langle\vec{\pi}\rangle$ of the pseudoscalar isotriplet field is equal to zero for isospin-symmetric systems.

The σ field has a non-vanishing vacuum expectation value as a consequence of spontaneous chiral symmetry breaking. Solving the field equations for σ, the effective quark mass m is determined by the self-consistent gap equation

$$m = m_0 - \langle\sigma\rangle = m_0 - G\langle\bar{\psi}\psi\rangle. \qquad (10)$$

Note that $\langle\sigma\rangle = G\langle\bar{\psi}\psi\rangle$ is negative in our representation, and the chiral (quark) condensate is $\langle\bar{\psi}\psi\rangle = \langle\bar{\psi}_u\psi_u + \bar{\psi}_d\psi_d\rangle$. For later purposes we note that Φ and $\bar{\Phi}$ are two independent field variables in the general case of finite quark chemical potential μ. They become equal in the limiting case $\mu = 0$. Their (thermal) expectation values $\langle\Phi\rangle$ and $\langle\bar{\Phi}\rangle$ are both real [56] but differ at non-zero μ.

---

[2]In the mean field approximation the fields are replaced by their expectation values for which, in later sections, we will continue using the notation σ, Φ and $\bar{\Phi}$ for simplicity and convenience.

a_0	a_1	a_2	a_3	b_3	b_4
6.75	-1.95	2.625	-7.44	0.75	7.5

Table 1: Parameter set used in this work for the Polyakov loop potential (5, 6).

Before passing to the actual calculations, we summarize basic assumptions behind eq. (1) and comment on limitations to be kept in mind. In fact the PNJL model (1) is quite schematic in several respects. It reduces gluon dynamics to a) chiral point couplings between quarks, and b) a simple static background field representing the Polyakov loop. This picture cannot be expected to work beyond a limited range of temperatures. At large T, transverse gluons are known to be thermodynamically active degrees of freedom, but they are ignored in the PNJL model. To what extent this model can reproduce lattice QCD thermodynamics is nonetheless a relevant question. We can assume that its range of applicability is, roughly, $T \leq (2 - 3)T_c$, based on the conclusion drawn in ref. [57] that transverse gluons start to contribute significantly for $T > 2.5\,T_c$.

3 Parameter fixing

3.1 Polyakov loop effective potential

The parameters of the Polyakov loop potential $\mathcal{U}$ are fitted to reproduce the lattice data [58] for QCD thermodynamics in the pure gauge sector. Minimizing $\mathcal{U}(\Phi, \bar{\Phi}, T)$ one has $\Phi = \bar{\Phi}$ and the pressure of the pure-gauge system is evaluated as $p(T) = -\mathcal{U}(T)$ with $\Phi(T)$ determined at the minimum. The entropy and energy density are then obtained by means of the standard thermodynamic relations. In Fig. 1 we show the (scaled) pressure, energy density and entropy density as functions of temperature. The lattice data are reproduced extremely well using the ansatz (5, 6), with parameters summarized in Table 1. The critical temperature T_0 for deconfinement appearing in Eq. (6) is fixed at $T_0 = 270$ MeV in the pure gauge sector. The resulting effective potential is displayed in Fig. 2 for two different temperatures: $T = 200$ MeV (below T_0) and $T = 320$ MeV (above T_0).

With the same parametrization, we are also able to reproduce the lattice data [59] for the temperature dependence of the Polyakov loop itself. A comparison between these data and our results is shown in Fig. 3. The Polyakov loop vanishes below the critical temperature T_0, at which point it jumps discontinuously to a finite value, indicating a first order phase transition. It tends to one at large temperatures, as expected.
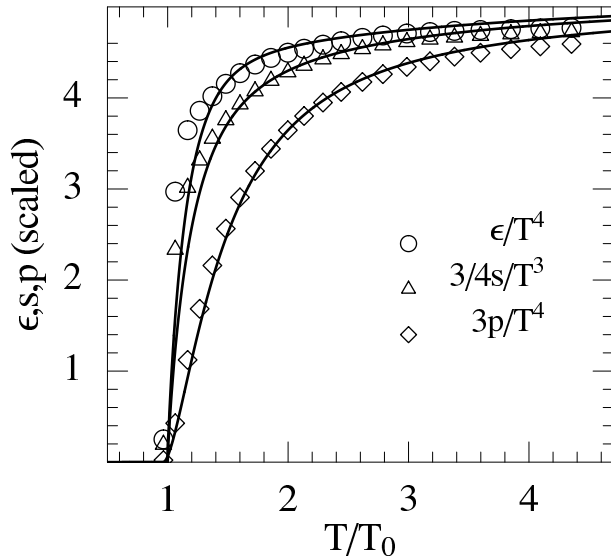
Figure 1: Scaled pressure, entropy density and energy density as functions of the temperature in the pure gauge sector, compared to the corresponding lattice data taken from Ref. [58].
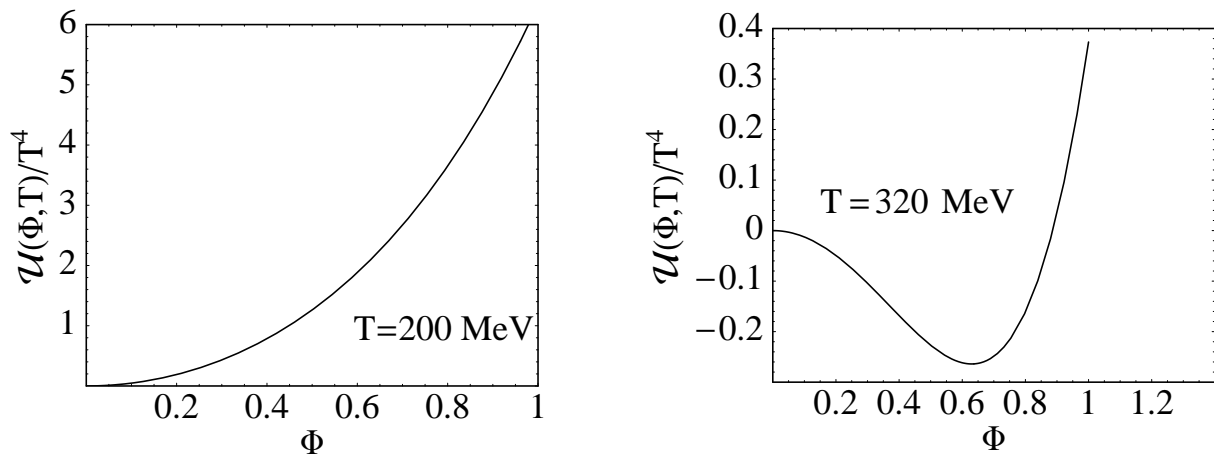

Figure 2: Scaled Polyakov loop effective potential $\mathcal{U}(\Phi, T)/T^4$ as a function of Φ for two values of temperature T.
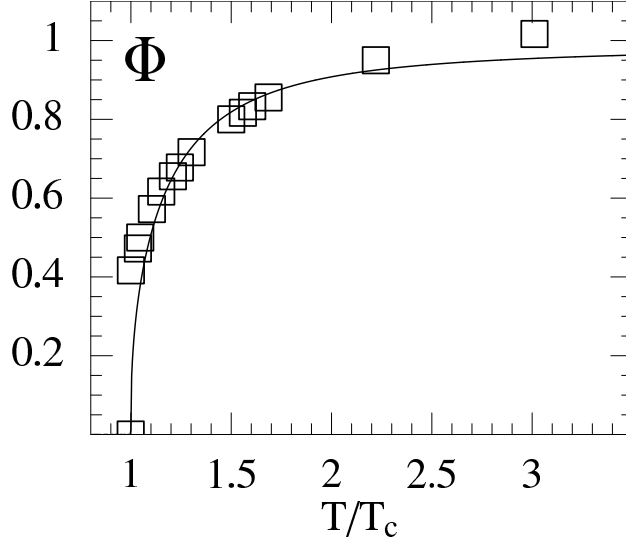
Figure 3:   Polyakov loop as a function of temperature in the pure gauge sector, compared to corresponding lattice results taken from Ref. [59].

3.2   NJL sector

The pure NJL model part of the Lagrangian (1) has the following parameters: the "bare" quark mass m_0, a three-momentum cutoff Λ and the coupling strength G. We choose to reproduce the known chiral physics in the hadronic sector at $T = 0$ and fix the three parameters by the following conditions:

- The pion decay constant is reproduced at its empirical value, $f_\pi = 92.4$ MeV. In the NJL model, f_π is evaluated using the following equation:

$$f_\pi^2 = 4m^2 I_\Lambda^{(1)}(m) \quad \text{where} \quad I_\Lambda^{(1)}(m) = -iN_c \int \frac{d^4p}{(2\pi)^4} \frac{\theta(\Lambda^2 - \vec{p}^{\,2})}{(p^2 - m^2 + i\epsilon)^2}, \quad (11)$$

  with the effective (constituent) quark mass m determined self-consistently by the gap equation (10).

- The quark condensate becomes

$$\langle \bar{\psi}_u \psi_u \rangle = -4m \, I_\Lambda^{(0)}(m) \tag{12}$$

  with

$$I_\Lambda^{(0)}(m) = iN_c \int \frac{d^4p}{(2\pi)^4} \frac{\theta(\Lambda^2 - \vec{p}^{\,2})}{p^2 - m^2 + i\epsilon}. \tag{13}$$

  Its "empirical" value derived from QCD sum rules is

$$\langle \bar{\psi}_u \psi_u \rangle^{1/3} \simeq \langle \bar{\psi}_d \psi_d \rangle^{1/3} = -(240 \pm 20) \text{ MeV}. \tag{14}$$

8

Λ [GeV]	$G[\mathrm{GeV}^{-2}]$	$m_0[\mathrm{MeV}]$
0.651	10.08	5.5
$|\langle \bar{\psi}_u \psi_u \rangle|^{1/3}[\mathrm{MeV}]$	$f_\pi[\mathrm{MeV}]$	$m_\pi[\mathrm{MeV}]$
251	92.3	139.3

Table 2: Parameter set used in this work for the NJL model part of the effective Lagrangian (1), and the resulting physical quantities. For these values of the parameters we obtain a constituent quark mass $m =$325 MeV.

- The current quark mass m_0 is fixed from the Gell-Mann, Oakes, Renner (GMOR) relation which is satisfied in the NJL model:

$$m_\pi^2 = \frac{-m_0 \left\langle \bar{\psi}\psi \right\rangle}{f_\pi^2} \ . \tag{15}$$

In the chiral limit, $m_0 = 0$ and $m_\pi = 0$.

The values of the NJL model parameters, together with the resulting physical quantities, are summarized in Table 2.

4   Results at finite T and μ

We now extend the model to finite temperature and chemical potentials using the Matsubara formalism. We consider the isospin symmetric case, with an equal number of u and d quarks (and therefore a single quark chemical potential μ). The quantity to be minimized at finite temperature is the thermodynamic potential per unit volume:

$$\Omega\left(T,\mu\right) \ = \ \mathcal{U}\left(\Phi, \bar{\Phi}, T\right) - \frac{T}{2}\sum_n \int \frac{d^3p}{(2\pi)^3} \mathrm{Tr} \ln \frac{\tilde{S}^{-1}\left(i\omega_n, \vec{p}\right)}{T} + \frac{\sigma^2}{2G}. \tag{16}$$

Here $\omega_n = (2n+1)\pi T$ are the Matsubara frequencies for fermions. The inverse quark propagator (in Nambu-Gorkov representation) becomes

$$\tilde{S}^{-1}\left(p^0, \vec{p}\right) = \begin{pmatrix} \gamma_0 p^0 - \vec{\gamma}\cdot\vec{p} - m - \gamma_0\left(\mu + iA_4\right) & 0 \\ 0 & \gamma_0 p^0 - \vec{\gamma}\cdot\vec{p} - m + \gamma_0\left(\mu + iA_4\right) \end{pmatrix}. \tag{17}$$

Using the identity $\mathrm{Tr}\ln(X) = \ln\det(X)$ we reduce the trace in (16) and find:

$$
\begin{aligned}
\Omega \;=\; & \mathcal{U}\left(\Phi, \bar{\Phi}, T\right) + \frac{\sigma^2}{2G} \\
& - 2N_f\, T \int \frac{\mathrm{d}^3 p}{(2\pi)^3} \left\{ \mathrm{Tr}_c \ln\left[1 + L\,\mathrm{e}^{-(E_p-\mu)/T}\right] + \mathrm{Tr}_c \ln\left[1 + L^\dagger\,\mathrm{e}^{-(E_p+\mu)/T}\right] \right\} \\
& - 6N_f \int \frac{\mathrm{d}^3 p}{(2\pi)^3} E_p\, \theta\left(\Lambda^2 - \vec{p}\,^2\right)
\end{aligned}
\tag{18}
$$

where we have introduced the quark quasiparticle energy $E_p = \sqrt{\vec{p}\,^2 + m^2}$. The last term involves the NJL three-momentum cutoff Λ. The second (finite) term does not require any cutoff. A small violation of the underlying chiral symmetry at $T > 0.4$ GeV, resulting from this procedure, is of no practical relevance since the model is supposed to be applied only at temperatures and chemical potential well below Λ.

The remaining colour trace is then performed with the result

$$
\begin{aligned}
& \ln\det\left[1 + L\,\mathrm{e}^{-(E_p-\mu)/T}\right] + \ln\det\left[1 + L^\dagger\,\mathrm{e}^{-(E_p+\mu)/T}\right] \\
=\; & \ln\left[1 + 3\left(\Phi + \bar{\Phi}\mathrm{e}^{-(E_p-\mu)/T}\right)\mathrm{e}^{-(E_p-\mu)/T} + \mathrm{e}^{-3(E_p-\mu)/T}\right] \\
+\; & \ln\left[1 + 3\left(\bar{\Phi} + \Phi\mathrm{e}^{-(E_p+\mu)/T}\right)\mathrm{e}^{-(E_p+\mu)/T} + \mathrm{e}^{-3(E_p+\mu)/T}\right] .
\end{aligned}
\tag{19}
$$

From the thermodynamic potential (18) the equations of motion for the mean fields σ, Φ and $\bar{\Phi}$ are derived through

$$
\frac{\partial \Omega}{\partial \sigma} = 0 \;, \qquad \frac{\partial \Omega}{\partial \Phi} = 0 \;, \qquad \frac{\partial \Omega}{\partial \bar{\Phi}} = 0 \;.
\tag{20}
$$

This set of coupled equations is then solved for the fields as functions of temperature T and quark chemical potential μ.

Fig. 4(a) shows the chiral condensate together with the Polyakov loop Φ as functions of temperature at $\mu = 0$ where we find again $\Phi = \bar{\Phi}$. One observes that the introduction of quarks coupled to the σ and Φ fields turns the first-order transition seen in pure-gauge Lattice QCD into a continuous crossover. The original 1st order transition in the pure-gauge system appears at a critical temperature $T_0 = 270$ MeV. With the introduction of quarks, the crossover transitions for the chiral condensate $\langle\bar{\psi}\psi\rangle$ and for the Polyakov loop perfectly coincide at a lower critical temperature $T_c \simeq 220$ MeV (see Fig. 4(b)). We point out that this feature is obtained without changing a single parameter with respect to the pure gauge case. The value of the critical temperature that we obtain is a little high if compared to the available data for two-flavour Lattice QCD [60] which gives $T_c = (173 \pm 8)$ MeV. On the other hand, it is presently being discussed that detailed continuum extrapolation of these data can increase this temperature up to 210 MeV [61]. For quantitative comparison
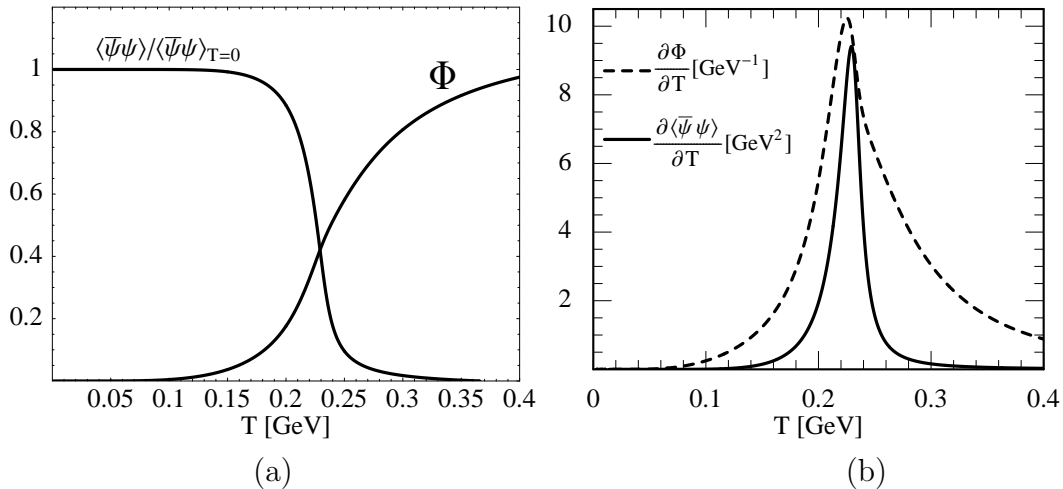
Figure 4: Left: scaled chiral condensate and Polyakov loop $\Phi(T)$ as functions of temperature at zero chemical potential. Right: plots of $\partial\langle\bar{\psi}\psi\rangle/\partial T$ and $\partial\Phi/\partial T$.

with existing lattice results we choose to reduce T_c by rescaling the parameter T_0 from 270 to 190 MeV. In this case we loose the perfect coincidence of the chiral and deconfinement transitions, but they are shifted relative to each other by less than 20 MeV. When defining T_c in this case as the average of the two transition temperatures we find $T_c = 180$ MeV. This is also consistent with the observations reported in [62].

As we turn to non-zero chemical potential, we find that Φ and $\bar{\Phi}$ are different from each other, even if they are both real. They will finally coincide again at high temperatures, as can be seen in Fig. 5. This feature was already observed in [56].

With increasing chemical potential, the crossover pattern evolves to lower transition temperatures (see Fig. 6) until it turns to a first order transition around $\mu \sim 0.3$ GeV. At this point Cooper pairing of quarks presumably sets in. A more detailed discussion of the critical point and its neighbourhood therefore requires the additional incorporation of explicit diquark degrees of freedom in the PNJL model. Further developments along these lines will be reported elsewhere.

5 Detailed comparison with Lattice QCD

A primary aim of this work is to compare predictions of our PNJL model with the lattice data available for full QCD thermodynamics at zero and finite μ. Consider first the pressure of the quark-gluon system at zero chemical potential:

$$p\left(T, \mu = 0\right) = -\Omega\left(T, \mu = 0; \sigma(T,0), \Phi(T,0), \bar{\Phi}(T,0)\right), \qquad (21)$$
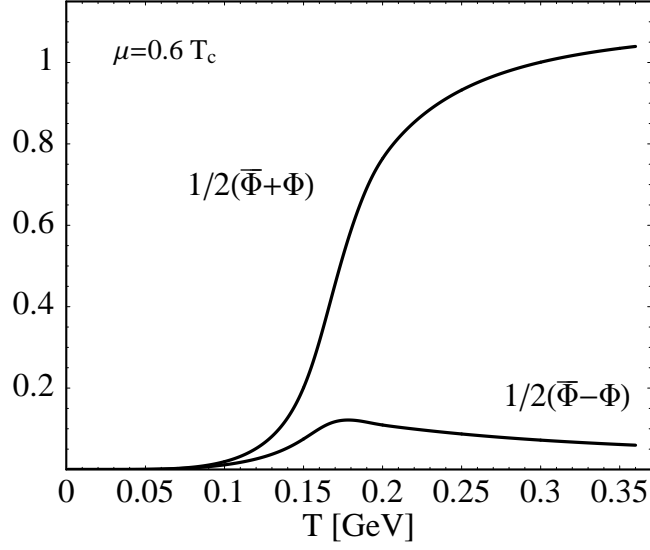
Figure 5: Averaged sum and difference of Φ and $\bar{\Phi}$ as functions of the temperature at finite μ.
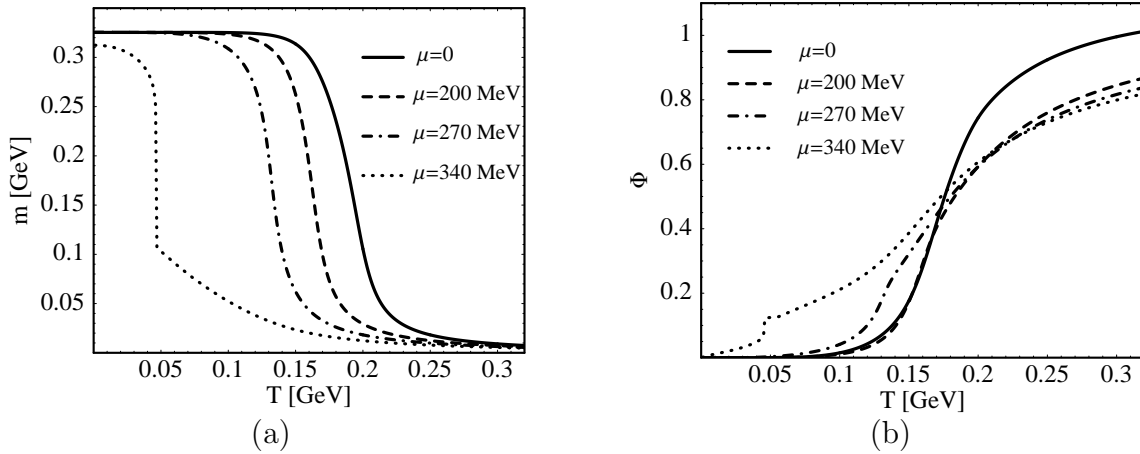

Figure 6: Constituent quark mass (a) and Polyakov loop (b) as functions of temperature for different values of the chemical potential.

where $\sigma\left(T,0\right)$, $\Phi\left(T,0\right)$ and $\bar{\Phi}\left(T,0\right)$ are the solutions of the field equations at finite temperature and zero quark chemical potential. Our results are presented in Fig. 7(a) in comparison with corresponding lattice data. We point out that the input parameters of the PNJL model have been fixed independently in the pure gauge and hadronic sectors, so that our calculated pressure is a prediction of the model, without any further tuning of parameters. With this in mind, the agreement with lattice results is quite satisfactory. One must note that the lattice data are grouped in different sets obtained on lattices with temporal extent $N_t = 4$ and $N_t = 6$, both of which are not continuum extrapolated. In contrast, our calculation should, strictly speaking, be compared to the continuum limit. In order to perform meaningful comparisons, the pressure is divided by its asymptotic high-temperature (Stefan-Boltzmann) limit for each given case. At high temperatures our predicted curve should be located closer to the $N_t = 6$ set than to the one with $N_t = 4$. This is indeed the case. Furthermore, Fig. 7(b) shows the predicted "interaction measure", $(\varepsilon - 3p)/T^4$, in comparison with lattice data for $N_t = 6$. One should of course note that the lattice results have been produced using relatively large quark masses, with pseudoscalar-to-vector mass ratios m_{PS}/m_V around 0.7, whereas our calculation is performed with light quark masses corresponding to the physical pion mass. We have investigated the dependence of the pressure and of the energy density on the quark mass and found that the critical temperature scales approximately as $T_c \simeq T_c(m_\pi = 0) + 0.04\, m_\pi$, in agreement with the behaviour found in [60]. Once the rescaling of T_c is taken into account, the curves plotted in Figs. 7(a) and 7(b) as functions of T/T_c have negligible remaining dependence on the quark mass.

At non-zero chemical potential, quantities of interest that have become accessible in Lattice QCD are the "pressure difference" and the quark number density. The (scaled) pressure difference is defined as:

$$\frac{\Delta p\left(T,\mu\right)}{T^4} = \frac{p\left(T,\mu\right) - p\left(T,\mu = 0\right)}{T^4}. \tag{22}$$

A comparison of Δp, calculated in the PNJL model, with lattice results is presented in Fig. 8. This figure shows the scaled pressure difference as a function of the temperature for a series of chemical potentials, with values ranging between $\mu = 0.2\, T_c^{(0)}$ and $\mu \simeq T_c^{(0)}$. The agreement between our results and the lattice data is quite satisfactory.

A related quantity for which lattice results at finite μ exist, is the scaled quark number density, defined as:

$$\frac{n_q\left(T,\mu\right)}{T^3} = -\frac{1}{T^3}\frac{\partial\Omega\left(T,\mu\right)}{\partial\mu}. \tag{23}$$

Our results for n_q as a function of the temperature, for different values of the quark chemical potential, are shown in Fig. 9 in comparison with corresponding lattice data
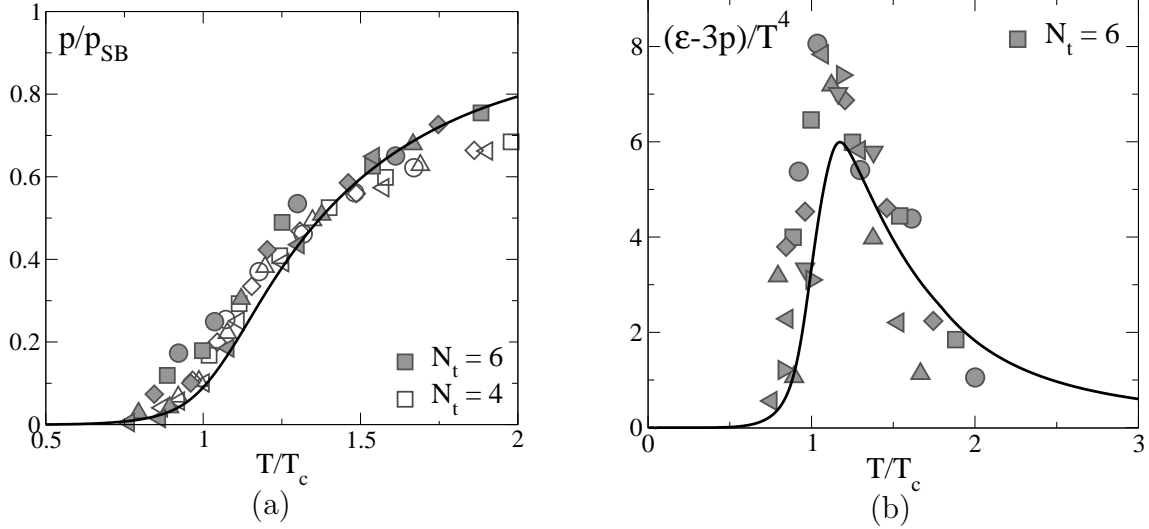
Figure 7: (a) Scaled pressure divided by the Stefan-Boltzmann (ideal gas) limit as a function of temperature at zero chemical potential: comparison between our PNJL model prediction and lattice results corresponding to $N_t = 4$ and $N_t = 6$. (b) Scaled interaction measure compared to lattice results for $N_t = 6$. In both cases, the lattice data are taken from Ref. [63]
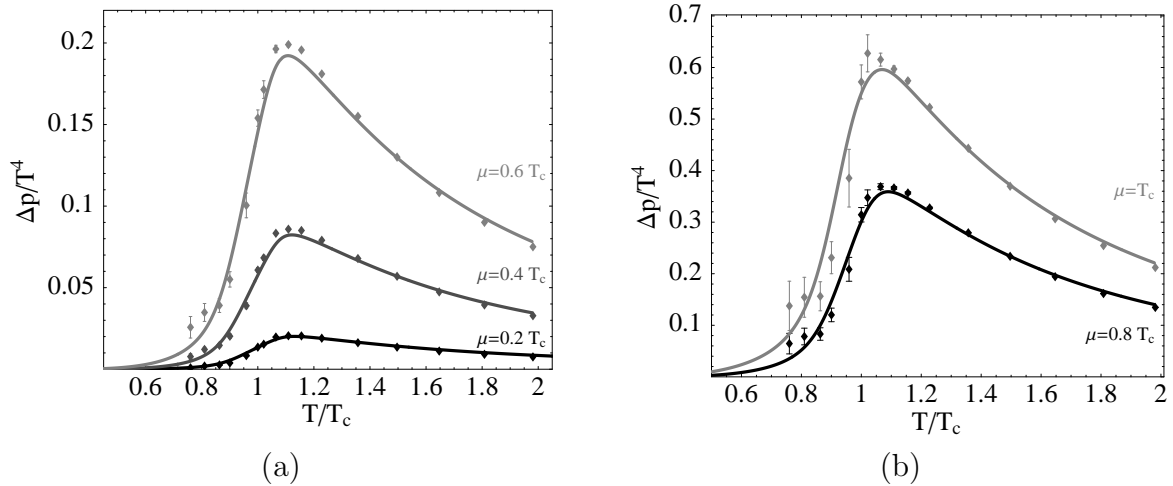

Figure 8: Scaled pressure difference as a function of temperature at different values of the quark chemical potential, compared to lattice data taken from Ref. [4].
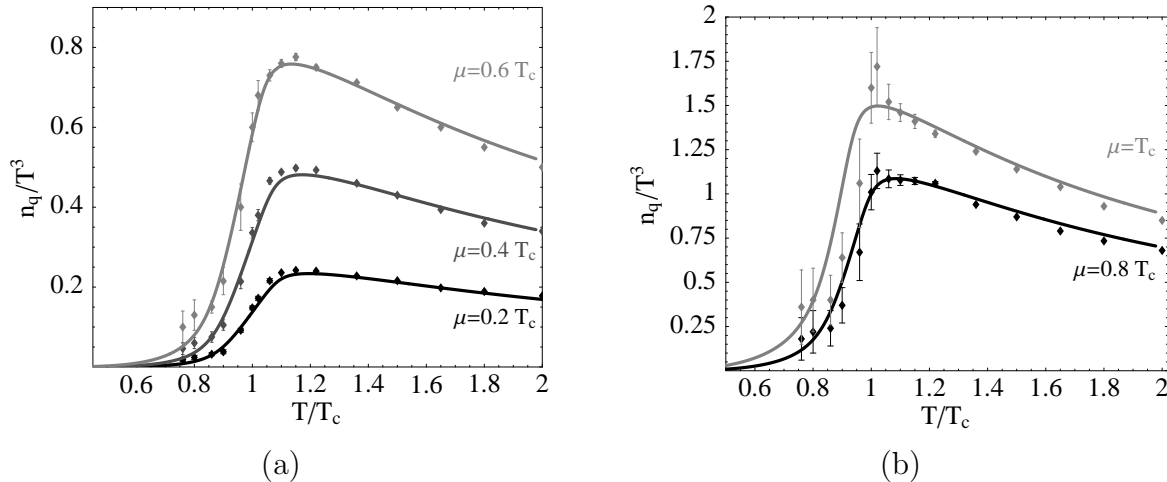
Figure 9: Scaled quark number densities as a function of temperature at different values of the chemical potential, compared to lattice data taken from Ref. [4].

[4]. Also in this case, the agreement between our PNJL model and the corresponding lattice data is surprisingly good.

It is instructive to study the effect of the Polyakov loop dynamics on the behaviour of the quark density n_q. The coupling of the quark quasiparticles to the field Φ reduces their weight as thermodynamically active degrees of freedom when the critical temperature T_c is approached from above. At T_c the value of Φ tends to zero and the quasiparticle exponentials $\exp[-(E_p \pm \mu)/T]$ are progressively suppressed in the thermodynamic potential as $T \to T_c$. This is what can be interpreted as the impact of confinement in the context of the PNJL model. In contrast, the standard NJL model without coupling to the Polyakov loop does not have this important feature, so that the quark density leaks strongly into the "forbidden" domain $T < T_c \simeq 170$ MeV, as demonstrated in Fig. 10.

It is a remarkable feature that the quark densities and the pressure difference at finite μ are so well reproduced even though the lattice "data" have been obtained by a Taylor expansion up to fourth order in μ, whereas our thermodynamic potential is used with its full functional dependence on μ. We have examined the convergence in powers of μ by expanding Eq.(18). It turns out that the Taylor expansion to order μ^2 deviates from the full result by less than 10 % even at a chemical potential as large as $\mu \sim T_c$. When expanded to $\mathcal{O}(\mu^4)$, no visible difference is left between the approximate and full calculations for all cases shown in Figs. 8 and 9.
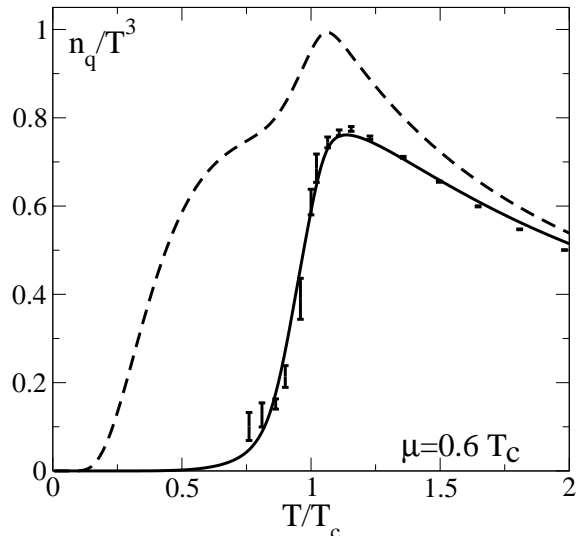
Figure 10: Comparison between the results in the PNJL model (solid line) and in the standard NJL model (dashed line) for the quark number density at $\mu = 0.6T_c$. The effect of the missing confinement is evident in the standard NJL model.

6 Summary and conclusions

We have studied a Polyakov-loop-extended Nambu and Jona-Lasinio (PNJL) model with the aim of exploring whether such an approach can catch essential features of QCD thermodynamics when confronted with results of lattice computations at finite temperature and non-zero quark chemical potential. This PNJL model represents a minimal synthesis of the two basic principles that govern QCD at low temperatures: spontaneous chiral symmetry breaking and confinement. The respective order parameters (the chiral quark condensate and the Polyakov loop) are given the meaning of collective degrees of freedom. Quarks couple to these collective fields according to the symmetry rules dictated by QCD itself.

Once a limited set of input parameters is fitted to Lattice QCD in the pure gauge sector and to pion properties in the hadron sector, the quark-gluon thermo-dynamics above T_c up to about twice the critical temperature is well reproduced, including quark densities up to chemical potentials of about 0.2 GeV. In particular, the PNJL model correctly describes the step from the first-order deconfinement transition observed in pure-gauge Lattice QCD (with $T_c \simeq 270$ MeV) to the crossover transition (with T_c around 200 MeV) when $N_f = 2$ light quark flavours are added. The non-trivial result is that the crossovers for chiral symmetry restoration and deconfinement almost coincide, as found in lattice simulations. The model also re-produces the quark number densities at various chemical potentials remarkably well when confronted with corresponding lattice data. Considering that the lattice results have been found by a Taylor expansion in powers of the chemical potential,

16

this excellent agreement came as a surprise and indicates rapid convergence of the power series in μ.

Further developments will be directed towards improvements to overcome some obvious limitations. First, the NJL model operates with a constant four-point coupling strength which supposedly averages the relevant running coupling over a limited low-energy kinematic domain, corresponding to temperatures $T \leq 2\,T_c$ and chemical potentials $\mu \leq 0.3$ GeV. Contacts with the high-temperature limit of QCD and the HTL approaches need to be established. Secondly, in order to proceed into the range of larger chemical potentials, diquark degrees of freedom need to be explicitly involved. Also, the effective potential for the Polyakov loop field, determined so far entirely as a function of temperature by investigating the pure gauge sector, must be examined with respect to its dependence on the chemical potential. And furthermore, the extension to 2+1 flavours with inclusion of strange quarks must be explored.

Nevertheless, considering the simplicity of the PNJL model, the conclusion that can be drawn at this point is promising: it appears that a relatively straightforward quasiparticle approach, with its dynamics rooted in spontaneous chiral symmetry breaking and confinement and with parameters controlled by a few known properties of the gluonic and hadronic sectors of the QCD phase diagram, can account for essential observations from two-flavour $N_c = 3$ Lattice QCD thermodynamics.

Acknowledgements

References

[1] Z. Fodor, S. D. Katz, and K. K. Szabo, Phys. Lett. B **568**, 73 (2003).

[2] Z. Fodor and S. D. Katz, JHEP **0203**, 014 (2002).

[3] C. R. Allton *et al.*, Phys. Rev. D **66**, 074507 (2002).

[4] C. R. Allton *et al.*, Phys. Rev. D **68**, 014507 (2003).

[5] C. R. Allton *et al.*, Phys. Rev. D **71**, 054508 (2005).

[6] E. Laermann and O. Philipsen, Ann. Rev. Nucl. Part. Sci. **53**, 163 (2003).

[7] P. de Forcrand and O. Philipsen, Nucl. Phys. B **673**, 170 (2003)

[8] M. D'Elia and M. P. Lombardo, Phys. Rev. D **67**, 014505 (2003).

[9] M. D'Elia and M. P. Lombardo, Phys. Rev. D **70**, 074509 (2004).

[10] P. Arnold and C. Zhai, Phys. Rev. D **51**, 1906 (1995).

[11] C. Zhai and B. Kastening, Phys. Rev. D **52**, 7232 (1995).

[12] E. Braaten and R. D. Pisarski, Phys. Rev. D **45**, R1827 (1992).

[13] J. Frenkel and J. C. Taylor, Nucl. Phys. B **374**, 156 (1992).

[14] J. P. Blaizot and E. Iancu, Nucl. Phys. B **417**, 608 (1994).

[15] J. O. Andersen, E. Braaten, and M. Strickland, Phys. Rev. Lett. **83**, 2139 (1999).

[16] J. O. Andersen, E. Braaten, and M. Strickland, Phys. Rev. D **62**, 045004 (2000).

[17] J. O. Andersen, E. Braaten, E. Petitgirard, and M. Strickland, Phys. Rev. D **66**, 085016 (2002).

[18] J. P. Blaizot, E. Iancu, and A. Rebhan, Phys. Rev. Lett. **83**, 2906 (1999).

[19] J. P. Blaizot, E. Iancu, and A. Rebhan, Phys. Lett. B **470**, 181 (1999).

[20] J. P. Blaizot, E. Iancu, and A. Rebhan, Phys. Rev. D **63**, 065003 (2001).

[21] K. Kajantie, M. Laine, K. Rummukainen, and Y. Schröder, Phys. Rev. D **67**, 105008 (2003).

[22] J. P. Blaizot, E. Iancu, and A. Rebhan, Phys. Rev. D **68**, 025011 (2003).

[23] A. Ipp, A. Rebhan, and A. Vuorinen, Phys. Rev. D **69**, 077901 (2004).

[24] J. Engels, F. Karsch, and H. Satz, Phys. Lett. B **113**, 398 (1982).

[25] A. Peshier, B. Kämpfer, O. P. Pavlenko, and G. Soff, Phys. Rev. D **54**, 2399 (1996).

[26] P. Levai and U. Heinz, Phys. Rev. C **57**, 1879 (1998).

[27] A. Peshier, B. Kämpfer, and G. Soff, Phys. Rev. C **61**, 045203 (2000).

[28] K. K. Szabo and A. I. Toth, JHEP **06**, 008 (2003).

[29] M. Bluhm, B. Kämpfer, and G. Soff, J. Phys. G **31**, S1151 (2005).

[30] M. Bluhm, B. Kampfer and G. Soff, Phys. Lett. B **620** (2005) 131

[31] R. D. Pisarski, Phys. Rev. D **62**, 111501(R) (2000).

[32] A. Rebhan and P. Romatschke, Phys. Rev. D **68**, 025022 (2003).

[33] R. A. Schneider and W. Weise, Phys. Rev. C **64**, 055201 (2001).

[34] M. A. Thaler, R. A. Schneider, and W. Weise, Phys. Rev. C **69**, 035210 (2004).

[35] A. Drago, M. Gibilisco, and C. Ratti, Nucl. Phys. A **742**, 165 (2004).

[36] Y. B. Ivanov, V. V. Skokov, and V. D. Toneev, Phys. Rev. D **71**, 014005 (2005).

[37] F. Karsch, K. Redlich and A. Tawfik, Phys. Lett. B **571**, 67 (2003); Eur. Phys. J. C **29**, 549 (2003).

[38] D. H. Rischke, Prog. Part. Nucl. Phys. **52**, 197 (2004).

[39] Y. Nambu and G. Jona-Lasinio, Phys. Rev. **122**, 345 (1961).

[40] Y. Nambu and G. Jona-Lasinio, Phys. Rev. **124**, 246 (1961).

[41] U. Vogl and W. Weise, Prog. Part. Nucl. Phys. **27**, 195 (1991).

[42] S. P. Klevansky, Rev. Mod. Phys. **64**, 649 (1992).

[43] T. Hatsuda and T. Kunihiro, Phys. Rept. **247**, 221 (1994).

[44] M. Buballa, Phys. Rept. **407**, 205 (2005).

[45] P. N. Meisinger and M. C. Ogilvie, Phys. Lett. B **379**, 163 (1996).

[46] P. N. Meisinger, T. R. Miller, and M. C. Ogilvie, Phys. Rev. D **65**, 034009 (2002).

[47] K. Fukushima, Phys. Lett. B **591**, 277 (2004).

[48] A. Mocsy, F. Sannino and K. Tuominen, Phys. Rev. Lett. **92** (2004) 182302

[49] E. Megias, E. Ruiz Arriola and L. L. Salcedo, arXiv:hep-ph/0412308.

[50] C. Ratti and W. Weise, Phys. Rev. D **70**, 054013 (2004).

[51] A. M. Polyakov, Phys. Lett. B **72**, 477 (1978).

[52] L. Susskind, Phys. Rev. D **20**, 2610 (1979).

[53] B. Svetitsky and L. G. Yaffe, Nucl. Phys. B **210**, 423 (1982).

[54] B. Svetitsky, Phys. Rept. **132**, 1 (1986).

[55] K. Fukushima, Ann. Phys. **304**, 72 (2003).

[56] A. Dumitru, R. D. Pisarski and D. Zschiesche, Phys. Rev. D **72**, 065008 (2005)

[57] P. N. Meisinger, M. C. Ogilvie and T. R. Miller, Phys. Lett. B **585**, 149 (2004)

[58] G. Boyd *et al.*, Nucl. Phys. B **469**, 419 (1996).

[59] O. Kaczmarek, F. Karsch, P. Petreczky, and F. Zantow, Phys. Lett. B **543**, 41 (2002).

[60] F. Karsch, Lecture Notes in Phys. (Springer) **583**, 209 (2002); F. Karsch, F. Laermann and A. Peikert, Nucl. Phys. B **605**, 579 (2002).

[61] Z. Fodor, private communication.

[62] S. Digal, F. Laermann and H. Satz, Eur. Phys. J. C **18**, 583 (2001).

[63] A. Ali Khan *et al.* Phys. Rev. D **64**, 074510 (2001).